Journal of Systemics, Cybernetics and Informatics (2025) 23(2), 84-90
https://doi.org/10.54808/JSCI.23.02.84

Trend analysis of remotely sensed historical rainfall in the Olifants River watershed, South Africa

Matsela Tlhologelo NKOABELA
Department of Civil and Environmental Engineering and Building Science
University of South Africa
Pretoria, South Africa

Masengo ILUNGA
Department of Civil and Environmental Engineering and Building Science
University of South Africa
Pretoria, South Africa

ABSTRACT

This study investigates the presence of climate change in the temporal variations of historical rainfall by utilising satellite-based precipitation data from 1993 to 2023 for the Olifants River watershed. Data were derived from the Center for Hydrometeorology and Remote Sensing (CHRS) Rainsphere system. The historical annual mean rainfall was found to be 621.45 mm, with the highest and lowest values observed in the year 2000 and 2015, respectively. A notable declining trend in annual rainfall was identified, while seasonal data showed a declining rainfall trend in Spring. It was also revealed that the spatial rainfall distribution from CHRS Rainsphere had little in common with the one derived from the observed rainfall data provided by the South African Weather Service.

Keywords: Rainfall, trend, artificial intelligence, remote sensing, climate change.

1. INTRODUCTION

Climate change is a worldwide occurrence that significantly influences the Earth's hydrological cycle, resulting in alterations in precipitation frequencies and intensities. The Olifants Watershed, located within the provinces of Gauteng, Limpopo and Mpumalanga in South Africa, is particularly vulnerable to the impacts of climate change. A study by [1] investigated the impacts of climate change on water resources in a rural community within the Limpopo Province. The study highlighted community-based adaptation practices in response to water insecurity, underscoring the necessity for sustainable water management strategies. Similarly, the study by [2] evaluated the hydroclimatic extremes in the Limpopo basin, including the Olifants watershed, under changing climate conditions. Their research identified significant increases in the frequency and intensity of extreme precipitation events, which have profound implications for water resource management in the region. Moreover, the study by [3] investigated the effects of climate change on water availability in the Olifants watershed and proposed potential adaptation strategies**.** Access to accurate and reliable information on climate change is crucial to addressing and alleviating the adverse impacts of climate change on the environment and its inhabitants [4]. Satellite-based precipitation estimation techniques have become indispensable for evaluating climate change, offering valuable perspectives on precipitation patterns across extensive regions. This can enable setting well-informed adaptation strategies. In this perspective, the CHRS Rainsphere system, an artificial intelligence-based system is explored to understand hydrological changes in the Olifants watershed.

2. SATELLITE-BASED PRECIPITATION ESTIMATION CHRS RAINSPHERE: OVERVIEW

Historically, rain gauges were utilised to quantify precipitation within specific areas. Nevertheless, their ability to accurately capture the comprehensive spatial and temporal intricacies of intense precipitation events, such as hurricanes and convective storms, was constrained by their limited resolution. Furthermore, the sparse distribution of rain gauges introduced uncertainties in precipitation measurements, particularly in regions with a scarcity of gauges. This uneven distribution further compromised the precision of precipitation estimates, especially in areas characterised by complex terrain and climate [5,6]. Recent advancements in satellite-based precipitation estimation techniques have revolutionised climate change studies. The authors of [4] emphasised the importance of accurate and reliable climate data for managing the adverse impacts of climate change on the environment and society. Satellite-based techniques, such as the precipitation estimation from remotely sensed information using an artificial neural network (PERSIANN), provide continuous and high-resolution precipitation data, which are crucial for climate change assessment. Recent literature, including studies by [7] & [2], has focused on comparing satellite-based precipitation estimates with ground-based observations to emphasise the necessity of validation for accurate trend analysis. Where possible, [8] has evaluated satellite precipitation products compared with ground measurements for accuracy [8, 9]. It is concluded from recent hydrological studies for South Africa that satellite based precipitation data such as Climate Hazards Group InfraRed Precipitation with Station data (CHIRPS) could play a significant role for water resources research [9]. This was validated by [10].

3. CLIMATE CHANGE ANALYSIS

The Mann-Kendall test is a commonly utilised non-parametric technique for detecting monotonic trends in environmental, climatic, or hydrological data series [11]. It has been endorsed by the International Meteorological Organisation (IMO) as a valuable tool for identifying sudden changes and trends in climate variables [12]. This method is particularly effective in examining temporal trends in climate parameters like temperature, precipitation, and evapotranspiration. Researchers in various regions, including Ethiopia, China, and Indonesia, have utilised the Mann-Kendall test to investigate climate change impacts and trends [13-15].
The Mann-Kendall test is conducted to examine the null hypothesis of no trend in comparison to the alternative hypothesis suggesting the presence of either an increasing or decreasing trend [16, 17].
The Mann-Kendall test statistic is calculated as follows:

$$S = \sum_{i=1}^{n-1} \sum_{j=i+1}^{n} \mathrm{sign}(X_j - X_i), \qquad \text{Eq. (1)}$$

$$\mathrm{sign}(X_j - X_i) = \begin{cases} +1 & (X_j - X_i) > 0 \\ 0 & (X_j - X_i) = 0 \\ -1 & (X_j - X_i) < 0 \end{cases} \qquad \text{Eq. (2)}$$

When the S value is positive, it indicates an upward trend, whereas a negative value suggests a downward trend. The Z value is derived by computing the variance of the rainfall. The Variance (S) is computed as follows:

$$Var(S) = \frac{n(n-1)(2n+5) - \sum_{i=1}^{m} t_i(t_i-1)(2t_i+5)}{18} \qquad \text{Eq. (3)}$$

A tied group (m) is a set of rainfall data with the same value when the sample size is n>10. The normal Z test statistic is calculated by the equation:

$$Z = \frac{S \pm 1}{Var(S)^{1/2}} \qquad \text{Eq. (4)}$$

In this equation, the value of S-1 is utilised when S is greater than 0, the value of S+1 is employed when S is less than 0, and the value of Z is set to 0 when S equals 0. An increasing trend is indicated by a positive value of Z, whereas any other value suggests a declining trend.

4. DATA AVAILABILTY AND METHODS

Study area and data used

The Olifants watershed (Figure 1, see after Section 7) covers approximately 81,26 km² and is located in the northeastern region of South Africa in the provinces of Gauteng, Mpumalanga, and Limpopo. The watershed stretches between Longitude: (-26.000 S -22.000 S) and Latitude: (28.000 E 32.000 E). The Olifants River serves as a significant tributary of the Limpopo River, beginning at Trichardt, east of Johannesburg, Gauteng province. It then flows in a northeastern direction through Limpopo and Mpumalanga province before entering Mozambique and ultimately reaching the Indian Ocean [18,19]. The main tributaries of the Olifants River are the Letaba, Wilge, Elands and Ga-Selati Rivers on the left side, alongside the Steelpoort, Blyde Klaserie and Timbavati Rivers on the right side [20].
The historical rainfall data were downloaded from the CHRS Rainsphere portal and used in the analysis.

Methods

The trend analysis of historical rainfall was carried out using the Mann-Kendall test as described in Section 3.
The test was done through CHRS Rainsphere artificial intelligence and enhanced with the MAKESENS 1.0. software. The former gave a spatial distribution of S value, whereas the latter gave Z values and further details on the Mann-Kendall test.

5. RESULTS AND DISCUSSION

Annual rainfall

Figure 2 shows that the mean annual rainfall for the 30-year period considered was 621.45 mm. The highest recorded annual rainfall of 1195.48 mm occurred in the year 2000, while the lowest annual rainfall experienced in the watershed was 364.50 mm, recorded in the year 2015.

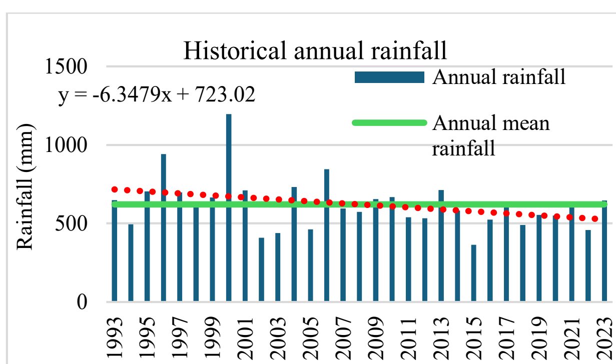

Figure 2. Historical annual rainfall for Olifants watershed

There are fluctuations in rainfall from year to year, with notable peaks occurring in the years 1996, 2000, 2001, 2004, 2006, and 2013 followed by notable lower rainfall values occurring in the years 1994, 2002, 2003, 2005, 2015, 2016, 2018, 2019, 2020, and 2022. The mean annual rainfall value is used to indicate the point of general stability in the average rainfall in the watershed; however, the persistent annual fluctuations from this mean highlight the watershed's vulnerability to both excessive rainfall and drought conditions. The linear equation ($y = -6.3479x + 723.02$) describes the negative trend in annual rainfall in the Olifants watershed. The summary of descriptive statistics of annual rainfall is presented in Table 1. These statistical parameters gave more insight into the variability and distribution of the rainfall events in the watershed. The mean and median annual rainfall were 621.45 mm and 620.15 mm, respectively, which suggests an approximately symmetrical distribution. However, a skewness of 1.55 suggests that there were more years with higher rainfall. A kurtosis of 4.25 indicates a leptokurtic distribution, which suggests that there was a higher occurrence of extreme rainfall events. The 26.25% coefficient of variation indicates moderate variability in the annual rainfall.

Table 1. Statistical parameters for historical annual rainfall for Olifants watershed

Statistical parameter	*Value*
Mean	621.45
Standard Error	29.29
Median	620.15
Mode	#N/A
Standard Deviation	163.10
Coefficient of Variation	26.25
Sample Variance	26602.54
Kurtosis	4.25
Skewness	1.55
Range	830.98
Minimum	364.50
Maximum	1195.48
Sum	19264.94
Count	31

Seasonal rainfall

The results for seasonal rainfall are shown in Figure 3 and Appendix 1.

For Autumn, the watershed experienced a mean rainfall of 123.76 mm, with a median of 113.97 mm. This indicates a right-hand skewness in the data, bolstered by a positive skewness value. The kurtosis value of -0.15 suggests a platykurtic distribution, implying a skewed distribution towards lower rainfall values. The coefficient of variance of 43.80% indicates moderate-high variability in rainfall during this season.

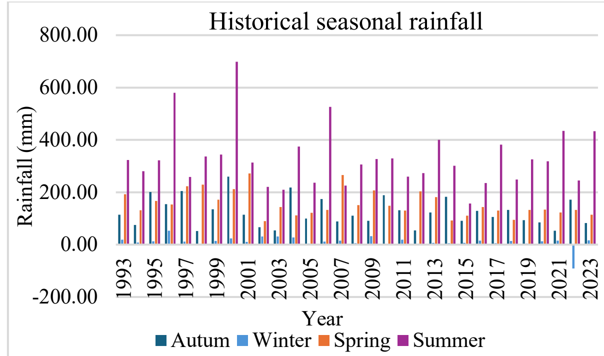

Figure 3. Historical seasonal rainfall for Olifants watershed.

The winter season experienced the least rainfall in comparison to the other seasons. The season's mean rainfall was 11.30 mm with a median of 12.34 mm indicative of a dry season. The negative skewness value of -3.21 suggests that there are occurrences of significantly low rainfall. The kurtosis value of 16.15 indicates a leptokurtic distribution, which suggests higher occurrence of extreme rainfall events in comparison to normal distribution. The coefficient of variation of 195.25% is indicative of very high variability, which suggests erratic and unpredictable rainfall patterns.

Spring exhibits characteristics of a much wetter season in comparison to the preceding seasons (autumn and winter). During the spring season, the watershed experienced a mean rainfall of 156.38 mm and a median of 143.32 mm, suggesting an almost symmetrical distribution. Additionally, the positive skewness value of 0.87 indicates a slight skew to the right, suggesting that there are fewer years with higher rainfall. Moreover, the kurtosis value of 0.08 is indicative of leptokurtic distribution, which suggests that there was a high occurrence of rainfall events. However, its closeness to zero also suggests that the distribution was close to normal distribution. The coefficient of variation of 30.98% is indicative of moderate variability in rainfall during this season.

Summer experiences the most rain in comparison to the other seasons. The season experienced a mean rainfall of 330.01 mm with a median of 318.29 mm. The skewness value of 1.54 shows that there were more years with higher rainfall. The kurtosis value of 3.062 shows a leptokurtic distribution, which means that extreme rainfall events happened more often than with a normal distribution. The coefficient of variation of 34.35% is indicative of moderate variability, which suggests consistent rainfall patterns and variations.

Trend analysis

The results of the trend analysis of historical rainfall are presented in Figure 4 (See after Section 7). The values of S parameter by Mann-Kendall suggested that rainfall patterns in the watershed remained stable with no evidence of a long-term upward or downward trend.

The MAKESENS 1.0. software gave more details on the significance of rainfall trend, as shown in Appendix 2.

The results indicate that the Olifants watershed experienced a statistically significant decreasing trend at 95% confidence in March and November with Z-values of -2.11 and -2.31, respectively, and a Sen slope (Q-value) of -1.34 and -1.27, respectively. The month of October experienced a statistically significant decreasing trend at 90% confidence with a Z-value of -1.84 and a Q-value of -0.79. The remaining months experienced a non-significant trend.

The seasons of autumn, winter, and summer indicate a non-significant trend, while spring indicates a significant decreasing trend at 95% confidence with a Z-value of -2.38 and a Q-value of -0.65.

The annual rainfall indicates a decreasing trend at 90% significance with a Z-value of -1.77 and a Q-value of -0.45. In terms of annual rainfall in the Olifants watershed, [21] reported a mean annual rainfall of 664 mm, with a standard deviation of 156.40 mm and a coefficient of variation of 24%. In contrast, [3] reported a wider range of mean annual rainfall ranging from 500-800 mm, with no standard deviation or coefficient of variation reported. This study recorded a slightly lower mean annual rainfall of 621.45 mm, with a standard deviation of 163.10 mm and a coefficient of variation of 26.25%, which is slightly higher than the coefficient of variability reported by [21]. Both studies [21, 22] corroborated the findings of this study by highlighting the variability in rainfall as well as high variability in seasonal rainfall in the Limpopo Province. Additionally, [22] noted that the region experiences its highest rainfall season during the summer, which further corroborates the results of seasonal rainfall observed in this study.

6. CONCLUSION

The study of rainfall data is valuable in identifying variations in frequency and intensity, which is crucial for essential sectors such as water management and agriculture. This study analysed rainfall patterns for a 30-year historical period and a 30-year future projected period in the Olifants Watershed in Limpopo, South Africa. This study utilised precipitation estimation from remotely sensed information using artificial neural networks (PERSIANN), specifically the Rainsphere dataset. Additionally, statistical parameters and the Mann-Kendall trend test were utilised to assess the variability and significance of trends in the rainfall over time. The analysis showed a historical annual mean rainfall of 621.45 mm, with notable peaks observed in the year 2000 and lows observed in the year 2015. A notable declining trend in annual rainfall was identified and confirmed by the Mann-Kendal trend test, while seasonal analysis shows a declining rainfall trend in spring.

7. REFERENCES

[1] Rankoana, S. A. (2020). Climate change impacts on water resources in a rural community in Limpopo Province, South Africa: A community-based adaptation to water insecurity. International Journal of Climate Change Strategies and Management, 12(1), 56-71.

[2] Botai, C. M., Botai, J. O., Zwane, N., Hayombe, P. O., Wamiti, E. K., Makgoale, T., & Tazvinga, H. (2020). Hydroclimatic extremes in the Limpopo Watershed, South Africa, under changing climate. Water, 12(12), 3299. https://doi.org/10.3390/w12123299

[3] Olabanji, M. F., Ndarana, T., Davis, N., & Archer, E. (2020). Climate change impact on water availability in the Olifants catchment (South Africa) with potential adaptation strategies. Physics and Chemistry of the Earth, 118, 102939.

[4] Abbas, M., Khan, F., Liou, Y., Ullah, H., Javed, B., & Ali, S. (2024). Assessment of the impacts of climate change on the construction of homogeneous climatic regions and ensemble climate projections using cmip6 data over Pakistan. Atmospheric Research, 304, 107359. https://doi.org/10.1016/j.atmosres.2024.107359

[5] Tessema, K. B., Haile, A. T., Amencho, N. W., & Habib, E. (2020). Effect of rainfall variability and gauge representativeness on satellite rainfall accuracy in a small upland watershed in southern Ethiopia. Hydrological Sciences Journal, 67(16), 2490–2504. https://doi.org/10.1080/02626667.2020.1770766

[6] Diodato, N., Tartari, G., & Bellocchi, G. (2010). Geospatial rainfall modelling at eastern Nepalese highland from ground environmental data. Water Resources Management, 24(11), 2703-2720. https://doi.org/10.1007/s11269-009-9575-2.

[7] Rachidi, S., Mazoudi, E. H. E., Alami, J. E., Jadoud, M., & Er-Raki, S. (2023). Assessment and comparison of satellite-based rainfall products: validation by hydrological modeling using ANN in a semi-arid zone. Water, 15(11), 1997. https://doi.org/10.3390/w15111997

[8] Tedla, M. G., Rasmy, M., Koike, T., & Zhou, L. (2024). Evaluation of satellite precipitation products for real-time extreme river flow modeling in data-scarce regions.

[9] Pitman, W. V. (2021). Can CHIRPS fill the gap left by the decline in the availability of rainfall stations in Southern Africa? Water SA, 47(2), 162-171.

[10] Kibii, J. K., & Du Plessis, J. A. (2023). The application of CHIRPS-based Pitman modelling in South Africa. Physics and Chemistry of the Earth, Parts A/B/C, 132, 103475.

[11] Yaouba, B. & Bitondo, D. (2022). Analysis of rainfall dynamics in the three main cities of Northern Cameroon. https://doi.org/10.21203/rs.3.rs-1757088/v1

[12] He, B., Sheng, Y., Cao, W., & Wu, J. (2020). Characteristics of climate change in northern Xinjiang in 1961–2017, China. Chinese Geographical Science, 30(2), 249-265. https://doi.org/10.1007/s11769-020-1104-5

[13] Dechassa, C., Simane, B., & Alamerew, B. (2020). Analysis of farmers perceived and observed climate variability and change in the Didessa sub-basin, Blue Nile River, Ethiopia. African Journal of Agricultural Research, 15(2), 149-164.

[14] Paudel, B., Wang, Z., Zhang, Y., Kumar, M., & Paul, P. K. (2021). Climate change and its impacts on farmers' livelihood in different physiographic regions of the trans-boundary Koshi Watershed, central Himalayas. International Journal of Environmental Research and Public Health, 18(13), 7142. https://doi.org/10.3390/ijerph18137142

[15] Olabanji, M. F., Davis, N., Ndarana, T., Kuhudzai, A. G., & Mahlobo, D. (2021). Assessment of smallholder farmers' perception and adaptation response to climate change in the Olifants catchment, South Africa. Journal of Water and Climate Change, 12(7), 3388-3403.

[16] Ojo, O. & Ilunga, M. (2018). Application of non-parametric trend technique for estimation of onset and cessation of rainfall. Air Soil and Water Research, 11. https://doi.org/10.1177/1178622118790264.

[17] Aditya, F., Gusmayanti, E. & Sudrajat, J. (2021). Rainfall trend analysis using Mann-Kendall and Sen's slope estimator test in West Kalimantan', IOP Conference Series: Earth and Environmental Science, 893, 012006. doi:10.1088/1755-1315/893/1/012006.

[18] Nkhonjera, G. K., Dinka, M. O., & Woyessa, Y. E. (2021). Assessment of localized seasonal precipitation variability in the upper middle catchment of the Olifants River Basin. Journal of Water and Climate Change, 12(1), 250-264. https://doi.org/10.2166/wcc.2020.187.

[19] Talukder, A.R. (2019). Impacts of climate change on the hydrological regime in the Olifants River, South Africa. Electronic Thesis and Dissertations, 8180. Available at: https://scholar.uwindsor.ca/etd/8180

[20] Thomas, A. P. (2015). Modelling of spatially distributed surface runoff and infiltration in the olifants river catchment/water management area using gis. International Journal of Advanced Remote Sensing and GIS, 4(1), 828-862. https://doi.org/10.23953/cloud.ijarsg.81

[21] Gyamfi, C., Ndambuki, J. M., & Salim, R. W. (2016). A historical analysis of rainfall trend in the olifants basin in South Africa. Earth Science Research, 5(1), 129. https://doi.org/10.5539/esr.v5n1p129.

[22] Maluleke, P., Moeletsi, M. E., & Tsubo, M. (2023). Analysis of climate variability and its implications on rangelands in the Limpopo Province. Climate, 12(1), 2. https://doi.org/10.3390/cli12010002.

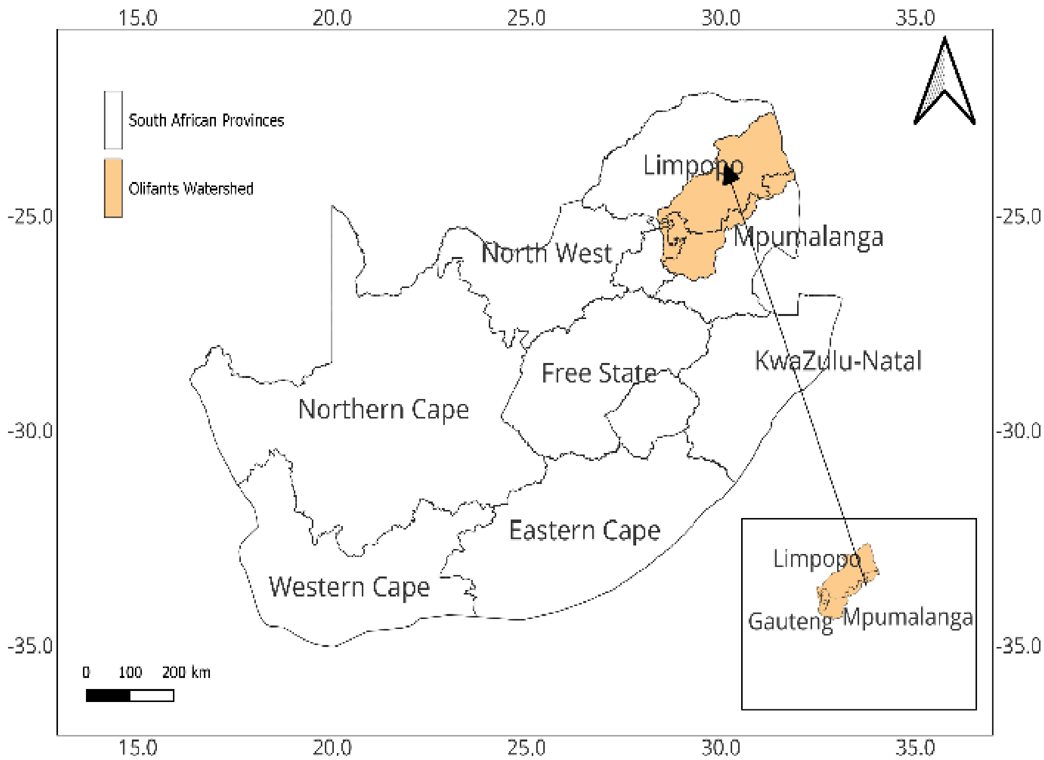

Figure 1. Olifants watershed study area location map.

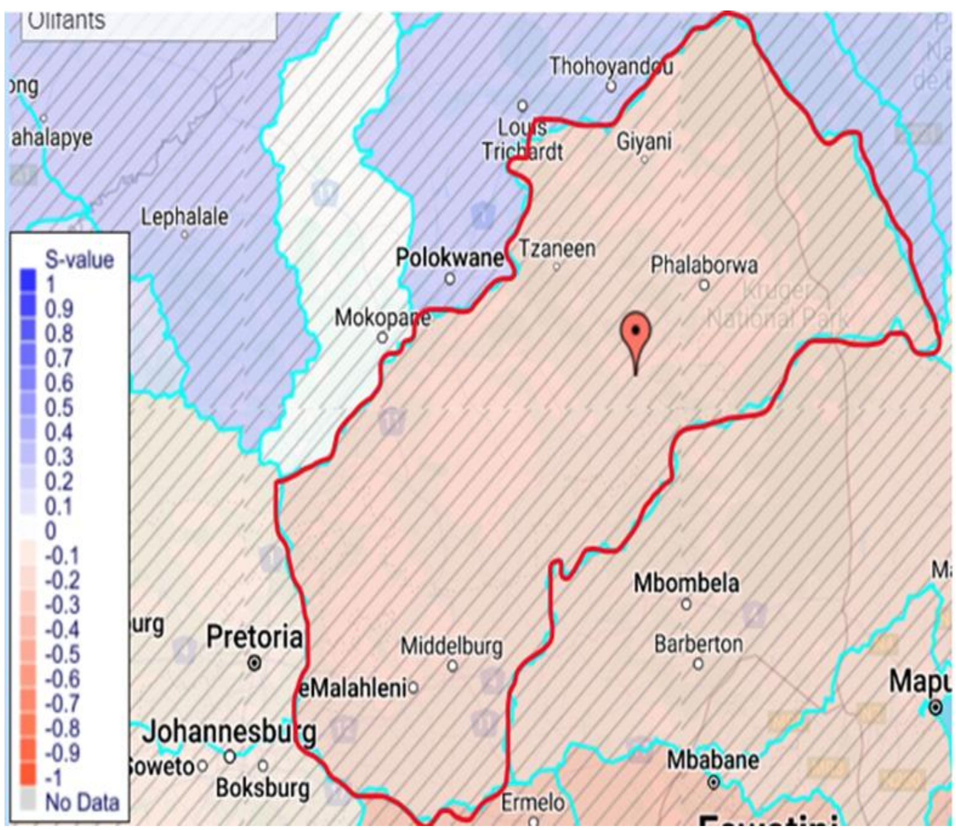

Figure 4. Mann-Kendal trend for Olifants watershed derived from CHRS Rainsphere.

Appendix 1. Statistical parameters for historical seasonal rainfall for Olifants watershed.

Statistical parameter	Autum	Winter	Spring	Summer
Mean	123.76	11.30	156.38	330.01
Standard Error	9.74	3.96	8.70	20.36
Median	113.97	12.34	143.32	318.29
Mode	90.64	#N/A	#N/A	#N/A
Standard Deviation	54.21	22.07	48.44	113.35
Coefficient of Variation	43.80	195.29	30.97	34.35
Sample Variance	2938.68	486.98	2346.36	12849.16
Kurtosis	-0.15	16.14	0.08	3.06
Skewness	0.70	-3.20	0.87	1.54
Range	208.67	144.52	181.57	541.87
Minimum	51.63	-91.01	90.34	157.01
Maximum	260.30	53.51	271.91	698.88
Sum	3836.52	350.29	4847.84	10230.29
Count	31.00	31.00	31.00	31.00

Appendix 2. Trend analysis for the period 1993-2023 for monthly rainfall for Olifants watershed. (min values of Q and B are not shown here)

Time series	Test Z	Signific.	Q	Qmax99	Qmax95	B	Bmax99	Bmax95
January	-0.24		-0.182	2.360	1.680	119.65	83.34	93.64
February	-0.41		-0.384	2.780	2.111	70.98	40.30	57.15
March	-2.11	*	-1.336	0.262	-0.101	76.43	54.26	58.57
April	0.14		0.176	1.354	1.011	31.64	19.64	24.24
May	-0.31		-0.046	0.756	0.531	8.99	0.91	2.93
June	-0.88		-0.064	0.100	0.054	3.23	1.06	1.81
July	0.32		0.013	0.217	0.172	2.45	-0.10	0.59
August	-1.00		-0.114	0.107	0.068	5.56	1.13	1.90
September	0.14		0.032	0.523	0.381	10.54	2.31	4.58
October	-1.84	+	-0.785	0.425	0.045	61.78	44.8047	51.0007
November	-2.31	*	-1.270	0.322	-0.430	116.19	84.3256	102.032
December	0.10		0.023	1.500	1.116	110.11	87.827	92.8197
Total annual rainfall	-1.77	+	-0.445	0.221	0.046	57.845	46.5505	50.8866
Autumnn	-1.14		-0.371	0.610	0.342	42.511	28.8604	34.2181
Winter	-1.26		-0.106	0.080	0.044	5.1997	2.81513	3.63914
Spring	-2.38	*	-0.652	0.037	-0.177	60.262	47.0867	49.5409
Summer	-0.20		-0.155	1.575	1.270	107.79	82.9401	88.1251